THE JOURNAL OF BIOLOGICAL CHEMISTRY VOL. 292, NO. 8, pp. 3517–3530, February 24, 2017

Genetic and Biochemical Characterization of a Gene Operon for *trans*-Aconitic Acid, a Novel Nematicide from *Bacillus thuringiensis*[*]

Received for publication, October 9, 2016, and in revised form, December 31, 2016 Published, JBC Papers in Press, January 13, 2017, DOI 10.1074/jbc.M116.762666

Cuiying Du[1], **Shiyun Cao**[1,2], **Xiangyu Shi, Xiangtao Nie, Jinshui Zheng, Yun Deng, Lifang Ruan, Donghai Peng, and Ming Sun**[3]

From the State Key Laboratory of Agricultural Microbiology, Huazhong Agricultural University, Wuhan 430070, China

Edited by Ruma Banerjee

trans*-Aconitic acid (TAA) is an isomer of *cis*-aconitic acid (CAA), an intermediate of the tricarboxylic acid cycle that is synthesized by aconitase. Although TAA production has been detected in bacteria and plants for many years and is known to be a potent inhibitor of aconitase, its biosynthetic origins and the physiological relevance of its activity have remained unclear. We have serendipitously uncovered key information relevant to both of these questions. Specifically, in a search for novel nematicidal factors from *Bacillus thuringiensis*, a significant nematode pathogen harboring many protein virulence factors, we discovered a high yielding component that showed activity against the plant-parasitic nematode *Meloidogyne incognita* and surprisingly identified it as TAA. Comparison with CAA, which displayed a much weaker nematicidal effect, suggested that TAA is specifically synthesized by *B. thuringiensis* as a virulence factor. Analysis of mutants deficient in plasmids that were anticipated to encode virulence factors allowed us to isolate a TAA biosynthesis-related (*tbr*) operon consisting of two genes, *tbrA* and *tbrB*. We expressed the corresponding proteins, TbrA and TbrB, and characterized them as an aconitate isomerase and TAA transporter, respectively. Bioinformatics analysis of the TAA biosynthetic gene cluster revealed the association of the TAA genes with transposable elements relevant for horizontal gene transfer as well as a distribution across *B. cereus* bacteria and other *B. thuringiensis* strains, suggesting a general role for TAA in the interactions of *B. cereus* group bacteria with nematode hosts in the soil environment. This study reveals new bioactivity for TAA and the TAA biosynthetic pathway, improving our understanding of virulence factors employed by *B. thuringiensis* pathogenesis and providing potential implications for nematode management applications.

Bacillus thuringiensis is an important entomopathogen that belongs to the *Bacillus cereus* group along with the human opportunistic pathogen *B. cereus* and mammalian etiological agent of anthrax *Bacillus anthracis* (1). Recent, research has classified *B. thuringiensis* as a bacterial pathogen of alternative nematode hosts (2–4), which may help to explain the complex ecology of *B. thuringiensis* that was previously thought to have a sole insect host (2, 5, 6). This finding further contextualizes already established interactions between *B. thuringiensis* and nematodes (1–4, 7), including free-living and parasitic species. The relationship between nematodes and *B. thuringiensis* is of great importance, because it not only gives new insights into the evolution and ecology of this important environmental microorganism (2, 3, 7) but also provides promising resources or strategies for nematode management.

B. thuringiensis bacterium is capable of undergoing a complete life cycle involving infection, germination, and reproduction stages inside *Caenorhabditis elegans* (1, 8). During the processes, a variety of virulence factors in nematicidal strains exhibit toxicity and cause the eventual death of the nematode host. Many important nematicidal factors of *B. thuringiensis* have been identified. Crystallized proteins, such as Cry5, Cry6, Cry13, Cry14, Cry21, and Cry55, are the predominant nematicidal toxins (8–15), and the application of Cry6A (16) or truncated Cry5B (17) in transgenic plants conferred significantly improved resistance to plant-parasitic nematodes. Meanwhile, chitinases (18), metalloproteinases (1, 4), lantibiotics (19), and a two-domain Nel protein (20) of *B. thuringiensis* are also active against nematodes. In addition to the most studied protein or peptide toxins, *B. thuringiensis* also secretes small active compounds to intoxicate nematodes. One identified compound in *B. thuringiensis* is thuringiensin, a 701-Da secondary metabolite that is highly synthesized and secreted by a 12-kb acyl carrier protein-dependent gene cluster (21). Thuringiensin displays excellent nematicidal activity against both free-living and plant-parasitic nematodes (22, 23). However, such small molecules are rarely reported in *B. thuringiensis*, leaving a gap in our understanding of the contributions of small molecular compounds to *B. thuringiensis* pathogenesis.

trans-Aconitic acid (TAA)[4] is a small unsaturated tricarboxylic acid that is a natural isomer of *cis*-aconitic acid (CAA) in the

[*] This work was supported by the China 948 Program of the Ministry of Agriculture (Grant 2016-X21), National Natural Science Foundation of China Grants 31670085 and 31171901, and National Key Research and Development Program of China Grant 2017YFC204521201. The authors declare that they have no conflicts of interest with the contents of this article.

[1] Both authors contributed equally to this work.

[2] Present address: Dept. of Microbiology and Cell Science, University of Florida, Gainesville, FL 32611.

[3] To whom correspondence should be addressed: State Key Laboratory of Agricultural Microbiology, Huazhong Agricultural University, Wuhan 430070, China. Tel.: 86-27-87283455; Fax: 86-27-87280670; E-mail: m98sun@mail.hzau.edu.cn.

[4] The abbreviations used are: TAA, *trans*-aconitic acid; CAA, *cis*-aconitic acid; TCA, tricarboxylic acid; TS, temperature-sensitive; J2s, second-stage juveniles; ACO, aconitase; SOE-PCR, splicing overlap extension PCR; ANOVA, analysis of variance; aa, amino acid(s).

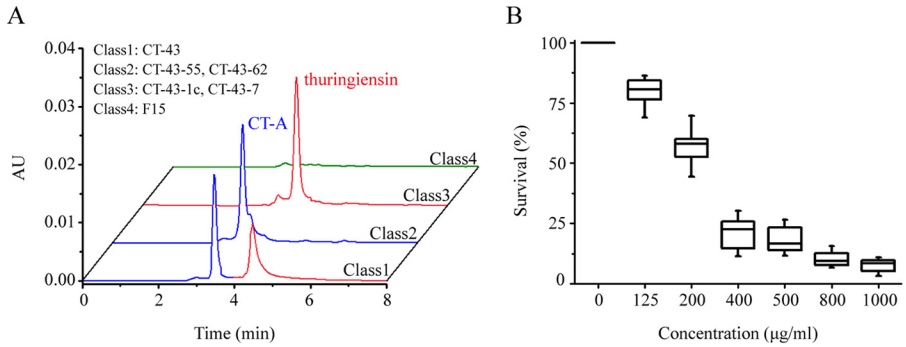

FIGURE 1. **The CT-A component prepared from *B. thuringiensis* CT-43-55 in class 2 showed nematicidal activity on the plant-parasitic nematode *M. incognita*.** *A*, classification of strain CT-43 and its plasmid-deficient mutants according to the production profile of CT-A (*blue peak*) and thuringiensin (*red peak*). The plasmid-deficient mutant CT-43-55 in class 2 is preferred for CT-A preparation over strains that produce thuringiensin. *B*, bioassay of a highly purified CT-A sample extracted from *B. thuringiensis* CT-43-55 on the J2s of the plant-parasitic root knot nematode *M. incognita*. The bioassay included three biological repeats, and treatment at each TAA concentration included three technological repeats. After 72 h, total and living J2s were counted and used to calculate the LC_{50} values by probit analysis (IBM SPSS software). *Error bars*, S.D. *AU*, absorbance units.

tricarboxylic acid (TCA) cycle (24). Although it is a strong inhibitor of aconitase in the TCA cycle (25, 26), TAA is highly produced by *Pseudomonas* bacteria (27, 28) and sugar-containing plants (29–31). It has been speculated that TAA can neutralize alkaline compounds absorbed by roots (32) and act as an antifeedant against the rice pest brown planthopper (33). However, these identified biological roles only partially explain the significance of naturally accumulated TAA, suggesting additional unrevealed biofunctions for TAA. Two TAA biosynthetic pathways have long been hypothesized: aconitate isomerase-mediated biosynthesis from a *cis*-aconitic acid substrate in both microbes (27, 28) and plants (29, 30), and a citric acid dehydratase-mediated synthesis reaction from citric acid substrate specific to maize (31). Although TAA is closely related to the central cellular metabolism of the TCA cycle, no exact genes have been identified as responsible for the *in vivo* formation of TAA.

In this study, we discovered that a thuringiensin-producing strain, *B. thuringiensis* CT-43 (34, 35), also highly produces the unusual cellular metabolite TAA. Bioassays conducted on nematodes revealed an unexpected lethal activity for TAA, suggesting that it is a novel nematicidal factor of the *B. thuringiensis* pathogen. Using genetic and biochemical techniques, we determined the TAA biosynthetic gene operon consisting of *tbrA* and *tbrB* genes in strain CT-43 as well as the isomerism and transportation processes mediated by aconitate isomerase TbrA and TAA transporter TbrB in the TAA biosynthesis of *B. thuringiensis*. Further, the distribution of the *tbr* operon across the *B. cereus* and *B. thuringiensis* strains indicated a general role for TAA in the interactions of bacteria with nematodes in soil environments.

Results

CT-A Is a Nematicidal Compound of B. thuringiensis CT-43—B. thuringiensis CT-43 (non-flagellum and previously classified as *B. thuringiensis* subsp. *chinensis*) (35) harbors 10 native plasmids carrying diverse toxic genes against nematode and insect targets (34). Thuringiensin is a nematicidal factor of strain CT-43, with a gene located on the pCT127 plasmid (21, 22). HPLC analysis of the culture supernatants of strain CT-43 and its plasmid-deficient mutants (35) showed different production profiles for thuringiensin and an undetermined high yielding compound, named CT-A. According to the production pattern, we divided these strains into four classes (Fig. 1*A*). To identify whether the highly produced CT-A was nematicidal, similar to thuringiensin, we prepared a highly purified sample of CT-A (Fig. 2*A*) from the culture supernatant of the thuringiensin-deficient mutant strain CT-43-55 in class 2 (Fig. 1*A*) by HPLC and conducted a bioassay on second-stage juveniles (J2s) of the root knot nematode *Meloidogyne incognita* (36), one of the most damaging plant-parasitic nematodes to global agriculture (37). As a result, the survival of *M. incognita* decreased with an increase in CT-A concentration (Fig. 1*B*). In particular, 44.1% of the population died when subjected to a low concentration (200 μg/ml); a moderate level of 400 μg/ml caused >78% mortality, and when CT-A level increased to 1,000 μg/ml, 92.1% of the nematodes died. The concentration at which 50% of *M. incognita* die (LC_{50}) after 72 h was calculated as 235.5 μg/ml using probit analysis (Fig. 1*B*). These results suggested that secreted CT-A was a nematicidal component of the *B. thuringiensis* CT-43.

The Nematicide CT-A Is trans-Aconitic Acid—To determine the structure of CT-A, the highly purified CT-A sample (Fig. 2*A*) was subjected to LC-Q-TOF-MS. The *m*/*z* 173.0090 ion representing the mass of the $[M - H]^-$ ion of the CT-A molecule is shown in Fig. 2*B*. Matching the signal of 173.0090 with METLIN, a metabolite mass spectral database (38), indicated that CT-A was aconitic acid ($C_6H_6O_6$, 174.11 Da), a known unsaturated tricarboxylic acid with two natural isomers: CAA and TAA (Fig. 3*A*). CAA and TAA commercial standards were analyzed by HPLC to determine whether CT-A is CAA or TAA, according to specific retention times. The CT-A peak was distinct from the CAA peak (Fig. 2*C*). However, the retention times of CT-A were consistent with those of the TAA standard under four tested mobile phase conditions (Fig. 2*D*), indicating that CT-A is TAA. NMR spectroscopy and IR spectroscopy revealing the internal structure of the CT-A molecule further confirmed this identification (data not shown).

To verify the nematicidal activity of the TAA molecule, we examined the effect of a commercial TAA standard on *M. incognita*. Nematode survival decreased as the TAA stan-

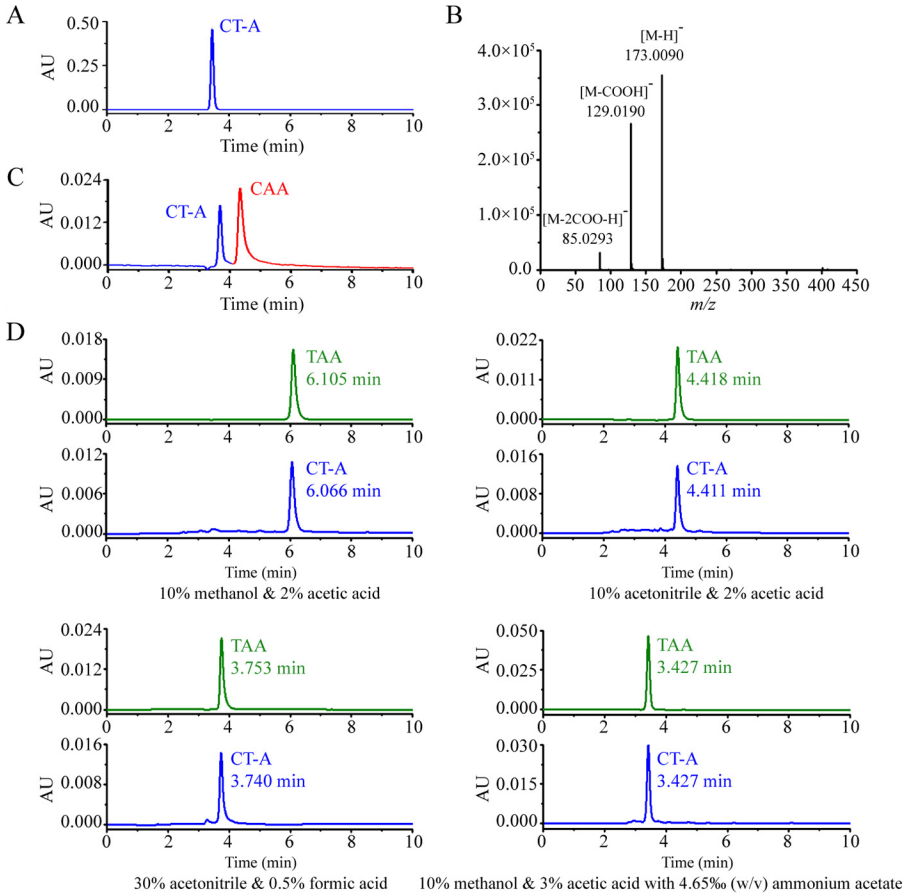

FIGURE 2. **Structure identification of CT-A molecule as *trans*-aconitic acid.** *A*, highly purified CT-A sample prepared from strain CT-43-55 by HPLC. *B*, Q-TOF-MS analysis of highly purified CT-A. The *m/z* 173.0090 ion represents the mass of the $[M - H]^-$ ion of CT-A. Analysis of the 173.0090 ion with the METLIN database revealed that CT-A was aconitic acid (*AA*). The *m/z* signals at 129.0190 and 85.0293 indicated the decarboxylation of one and two carboxyl groups from the $[M - H]^-$ ion, respectively. *C*, HPLC analysis of a mixed sample of CT-A extract from strain CT-43-55 and a CAA commercial standard showed two separated peaks. *D*, HPLC analysis of retention times of CT-A extract from strain CT-43-55 with a *trans*-aconitic acid (TAA) commercial standard under four different mobile phase conditions. The retention times and compositions of each mobile phase are provided. *AU*, absorbance units.

dard concentration increased, and the LC_{50} value of the TAA standard on *M. incognita* after 72 h was calculated as 226.3 μg/ml (Fig. 3*B*, *blue line*), which was consistent with that of the highly purified CT-A (Fig. 1*B*). These results demonstrated that TAA was a nematicide. CAA, whose pH value was similar to TAA (data not shown), showed a significantly higher LC_{50} value of 912.1 μg/ml (Fig. 3*B*, *red line*), ruling out the possibility that TAA kills nematodes mainly through its acidity. Overall, these results confirmed that the highly produced CT-A in *B. thuringiensis* CT-43 was TAA, a TCA cycle-related metabolite that displays a novel nematicidal bioactivity.

The Operon Consisting of tbrA and tbrB Genes Is Responsible for TAA Biosynthesis in B. thuringiensis CT-43—Before CT-A was identified as TAA, we presumed that it was another nematicidal secondary metabolite of *B. thuringiensis* CT-43 other than thuringiensis and began to isolate its biosynthesis genes within the CT-43 genome. Given that most of the toxins encoding genes in *B. thuringiensis* are plasmid-borne (21, 39), we first investigated the relationship of CT-A formation with plasmids present in various plasmid-deficient mutants of strain CT-43 to preliminarily locate CT-A biosynthesis genes (Table 1). As shown by mutants CT-43-55 and CT-43-62 in class 2, the deficiency of plasmid pCT127 affected the production of thuringiensin but not CT-A; in CT-43-1c (class 3), deficiency of only the pCT281 plasmid abolished CT-A production, and CT-43-7 (class 3) or F15 (class 4) whose pCT281 plasmid was absent also produced no CT-A. Together, these data indicated that CT-A biosynthesis-related genes were located on the biggest plasmid, pCT281 (281,231 bp; 276 genes), of strain CT-43. Because bioinformatics analysis of the pCT281 sequence with antiSMASH, a microbial secondary metabolite biosynthetic gene cluster database (40), showed no cluster targets, we adopted a full sequence-wide deletion strategy covering any possible compound biosynthesis-related genes on pCT281 (Table 2) and successfully deleted one acetyltransferase, one *N*-hydroxyarylamine *O*-acetyltransferase, and 11 hypothetical protein-encoding genes on pCT281 (Table 2) through a temperature-sensitive (TS) replicon-mediated homologous recombination method (21). No genes were CT-A biosynthesis-related, because CT-A production was not affected in these mutants (data not shown). However, both efficiencies of transformation in the wild strain CT-43 and homologous recombination via temperature stress on the TS replicon were confirmed to be low. We failed to target CT-A biosynthesis genes by this deletion strategy until CT-A was identified as the cellular metabolite TAA.

Although known for almost a century (25, 41), TAA biosynthesis genes and processes remain unclear *in vivo*. As mentioned above, aconitate isomerase has long been proposed to be

responsible for TAA biosynthesis in microbes by driving the interconversion between CAA and TAA (27, 28). However, no genes of aconitate isomerase have been genetically identified or can be referenced in the *B. thuringiensis* bacterium. Thus, we analyzed all of the genes in pCT281 using CD-Search (42) to identify isomerous function-related genes. Fortunately, we found the *CT43_RS29745* (1,074 bp) gene, which was the sole target of pCT281 (Fig. 4*A*) and showed sequence homology to the reported isomerase 2-methyl aconitate *cis*/*trans*-isomerase PrpF (43). The *CT43_RS29745* gene encodes a hypothetical protein whose sequence shared 27% identity and 97% coverage with that of PrpF (397 aa) in *Shewanella oneidensis* MR-1 (Fig. 4*B*) (43). Additionally, PrpF was speculated to catalyze the interconversion of 2-methyl CAA and 2-methyl TAA in the 2-methylcitric acid cycle (43, 44). Based on these findings, we proposed that *CT43_RS29745* is a gene encoding aconitate isomerase that is responsible for TAA biosynthesis in *B. thuringiensis* CT-43 and named it TAA biosynthesis-related gene *A* (*tbrA*). Meanwhile, another hypothetical protein-encoding gene, *tbrB* (*CT43_RS29750*, 912 bp), which was located 111 bp downstream of the *tbrA* and constituted an operon with *tbrA* (Fig. 4, *A* and *C*), also attracted our attention. Bioinformatics analysis of the TbrB protein showed an L-rhamnose-H^+ transporter (RhaT) domain (45, 46) and 10 transmembrane helices (Fig. 4*D*), indicating TbrB as a potential TAA transporter.

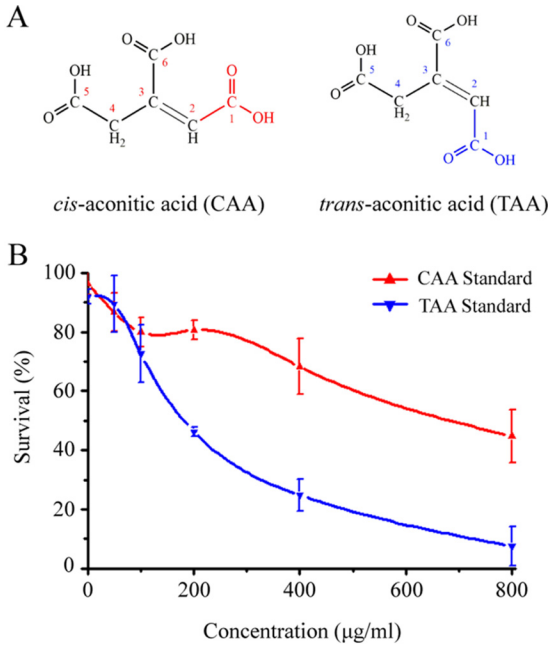

FIGURE 3. **TAA displayed much stronger nematicidal activity than CAA on J2s of *M. incognita*.** *A*, chemical structural formulas of CAA and TAA isomers. The conformational differences between the 1-carboxyl groups in CAA and TAA molecules are highlighted in *red* and *blue*, respectively. *B*, bioassays of CAA and TAA standards on J2s of *M. incognita*. Each bioassay included three biological repeats, and treatment for each concentration contained three technological repeats. After 72 h, the total and living numbers of J2s in CAA and TAA bioassays were recorded and used to calculate the LC_{50} values by probit analysis (IBM SPSS software). Data are means ± S.D. (*error bars*).

To test whether the operon comprising the *tbrA* and *tbrB* genes is responsible for TAA biosynthesis, we performed heterologous expression of the operon carried by the pHT304 vector (47) in *B. thuringiensis* BMB171 (48), an acrystalliferous *B. thuringiensis* mutant producing no TAA. This resulted in a recombinant termed BMB2451. HPLC and Q-TOF-MS analysis of the culture supernatant of BMB2451 confirmed TAA production (Fig. 5, *A* (*pink line*) and *B*). Subsequent gene deletions of *tbrA* and *tbrB* in the recombinant BMB2451 generated the recombinants BMB2451-Δ*tbrA* and BMB2451-Δ*tbrB*, respectively. TAA production was not observed in either supernatant by HPLC analysis (Fig. 5*A*, *dark green* and *blue lines*). When either *tbrA* or *tbrB* was complemented via another compatible vector pEMB0603 (39) in BMB2451-Δ*tbrA*:*tbrA* or BMB2451-Δ*tbrB*:*tbrB*, TAA production was restored (Fig. 5*A*, *red* and *black lines*). Together, these results genetically verified that the operon consisting of *tbrA* and *tbrB* was the TAA biosynthetic gene cluster of *B. thuringiensis* CT-43.

TbrA Protein Acts as Aconitate Isomerase in the Formation of TAA in B. thuringiensis—To verify the aconitate isomerase activity of TbrA protein, a TbrA-inducible *Escherichia coli* recombinant Rosetta-TbrA was constructed with the expression vector pET28a. After induction, the cell-free extracts of Rosetta-TbrA and Rosetta-pET28a (with empty vector only) were used for *in vitro* catalytic assays. First, we used CAA as a substrate to test TAA formation. Using a constant level of Rosetta-TbrA cell-free extract and a CAA concentration gradient from 2 to 20 mM, TAA formation was found to increase as CAA concentration increased. TAA formation was not detected in the Rosetta-pET28a cell-free extract (Fig. 6*A*). Meanwhile, when the CAA level was constant (10 mM), increasing the content of Rosetta-TbrA cell-free extract also resulted in increasing TAA formation. Rosetta-pET28a cell-free extract showed no enzymatic activity (Fig. 6*B*). These results demonstrated that TbrA could catalyze CAA into TAA. Next, we used

TABLE 1

Native plasmid distribution and CT-A (TAA) production in *B. thuringiensis* CT-43 and its plasmid-deficient mutants

Plus and minus signs indicate the presence and absence of relevant plasmid, respectively.

			Class 2		Class 3		
Plasmid	Size	Class 1: CT-43 (CT-A)	CT-43-55 (CT-A)	CT-43-62 (CT-A)	CT-43-1c (no CT-A)	CT-43-7 (no CT-A)	Class 4: F15 (no CT-A)
	bp						
pCT281	281,231	+	+	+	−	−	−
pCT127	127,885	+	−	−	+	+	−
pCT83	83,590	+	+	+	+	+	+
pCT72	72,074	+	+	+	+	+	+
pCT51	51,488	+	+	+	+	−	+
pCT14	14,860	+	+	+	+	+	+
pCT9547	9,547	+	+	+	+	+	+
pCT8513	8,513	+	+	+	+	+	+
pCT8252	8,252	+	+	+	+	+	+
pCT6880	6,880	+	+	+	+	+	+

TABLE 2

Design of full sequence-wide gene deletions in plasmid pCT281 of *B. thuringiensis* CT-43

The full sequence of plasmid pCT281 (~281 kb) was divided into 28 regions (every 10 kb from 0 to 281 kb). Primer locations in each region defined the deleted sequence range, within which certain genes that were functionally unidentified or predicted to be biosynthesis-related were targeted and described according to the National Center for Biotechnology Information (NCBI) database. The primer locations in *blue* and *red* represent the completed constructions of gene-knockout recombinant vectors and the further completed transformations of relevant vectors into strain CT-43, respectively. The targeted genes in *green* were successfully deleted genes.

Region (kb)	Primer location (bp)	Targeted gene (bp)	Annotation
0 – 10	4,531-5,689	*CT43_RS28695* (5,073-5,887)	Acetyltransferase
10 – 20	13,776-16,869	*CT43_RS28750* (14,637-15,479)	N-hydroxyarylamine O-acetyltransferase
20 – 30	20,514-25,397	*CT43_RS28780* (23,111-24,127)	Hypothetical protein
30 – 40	32,899-36,089	*CT43_RS28845* (33,847-35,151)	Large protein of pyocin AP41
40 – 50	40,970-42,448	*CT43_RS28875* (40,970-42,613)	Peptide ABC transporter substrate-binding protein
50 – 60	52,710-54,104	*CT43_RS28930* (53,158-53,949)	Glyoxalase
		CT43_RS28975 (59,909-60,838)	Membrane protein
60 – 70	—[a]		
70 – 80	71,325-76,273	*CT43_RS29025* (71,827-72,309)	Thiol reductase thioredoxin
		CT43_RS29030 (72,350-73,495)	Membrane protein
		CT43_RS29035 (73,952-74,635)	CAAX amino protease
		CT43_RS29040 (74,967-75,212)	Hypothetical protein
80 – 90	88,445-94,002	*CT43_RS29110* (87,914-91,933)	Hypothetical protein
90-100	92,971-98,351	*CT43_RS29130* (96,768-97,682)	Hypothetical protein
100 – 110	101,377-106,179	*CT43_RS29170* (101,904-102,701)	Hypothetical protein
110 – 120	109,853-116,412	*CT43_RS29230* (110,925-111,791)	Hypothetical protein
		CT43_RS29235 (111,793-112,725)	Hypothetical protein
		CT43_RS29240 (112,718-114,151)	Hypothetical protein
120 – 130	122,324-128,270	*CT43_RS29290* (123,493-124,440)	Hypothetical protein
		CT43_RS29295 (125,157-126,293)	Hypothetical protein
130 – 140	—		
140 – 150	142,687-150,992	*CT43_RS29365* (144,308-145,078)	Hypothetical protein
		CT43_RS29375 (146,293-147,219)	Hypothetical protein
		CT43_RS29380 (147,555-147,818)	Hypothetical protein
		CT43_RS29385 (147,969-148,159)	Hypothetical protein
		CT43_RS29390 (148,625-149,470)	Hypothetical protein
150 – 160	150,376-155,559	*CT43_RS29405* (150,990-151,547)	Hypothetical protein
		CT43_RS29410 (151,544-152,356)	Hypothetical protein
		CT43_RS29415 (152,386-153,207)	Hypothetical protein
		CT43_RS29420 (153,185-153,829)	Hypothetical protein
		CT43_RS29425 (153,878-154,843)	Hypothetical protein
160 – 170	161,598-167,065	*CT43_RS29470* (162,054-163,763)	Hypothetical protein
		CT43_RS29475 (164,450-165,919)	Hypothetical protein
170 – 180	—		
180 – 190	182,638-188,634	*CT43_RS29560* (185,210-185,389)	Hypothetical protein
		CT43_RS29565 (186,139-187,230)	SAM-dependent methyltransferase
		CT43_RS29570 (187,246-187,473)	Hypothetical protein
190 – 200	191,690-196,065	*CT43_RS29590* (193,761-194,474)	Hypothetical protein
		CT43_RS29595 (194,811-195,440)	Hypothetical protein
200 – 210	202,638-209,734	*CT43_RS29640* (203,322-203,966)	Hypothetical protein
		CT43_RS29655 (204,586-205,044)	Hypothetical protein
		CT43_RS29660 (205,035-205,472)	2-oxoglutarate dehydrogenase
		CT43_RS29670 (206,029-207,120)	Hypothetical protein
		CT43_RS29675 (207,428-207,745)	Hypothetical protein
		CT43_RS29680 (207,742-208,119)	Hypothetical protein
		CT43_RS29685 (208,203-208,718)	Hypothetical protein
210 – 220	210,307-215,631	*CT43_RS29700* (211,256-211,669)	Hypothetical protein
		CT43_RS29705 (212,066-212,881)	N-hydroxyarylamine O-acetyltransferase
220 – 230	221,829-227,128	*CT43_RS29750* (222,173-223,084)	Hypothetical protein
230 – 240	236,659-237,609	*CT43_RS29805* (236,659-237,609)	Membrane protein
240 – 250	237,424-243,455	*CT43_RS29815* (238,463-238,855)	Hypothetical protein
		CT43_RS29820 (239,175-240,491)	Amidohydrolase
		CT43_RS29825 (241,127-241,660)	Membrane protein
250 – 260	251,143-256,495	*CT43_RS29870* (252,117-254,486)	Hypothetical protein
		CT43_RS29880 (255,935-256,168)	Hypothetical protein
260 – 270	261,100-266,416	*CT43_RS29890* (261,048-262,778)	Methyl-accepting chemotaxis protein
		CT43_RS29895 (263,615-264,109)	Potassium transporter
		CT43_RS29900 (264,114-265,313)	Potassium transporter
270 – 281	274,668-279,260	*CT43_RS29925* (274,653-275678)	Appr-1-p processing protein
		CT43_RS29930 (275,693-276,325)	Hypothetical protein

[a] No genes were targeted in this region.

TAA as a substrate to test CAA formation. As shown, CAA was detected in cell-free extracts of Rosetta-TbrA but not Rosetta-pET28a (Fig. 6, *C* and *D*), which demonstrated that TbrA catalyzes a reversible reaction from CAA to TAA, and the equilibrium favors isomerization into TAA (Fig. 6, *E* and *F*). Moreover, *tbrA* deletion abolished *in vivo* TAA formation in mutant BMB2451-Δ*tbrA*, as observed by Q-TOF-MS analysis (Fig. 5*C*). Together, these results demonstrated that TbrA has aconitate isomerase activity that mediates TAA formation in *B. thuringiensis*.

TbrB Is a Membrane Transporter of TAA in B. thuringiensis—To determine the subcellular localization of TbrB, a putative membrane protein, we generated a fusion gene construct by connecting *tbrB* ORF to the green fluorescent protein (*gfp*) gene under the control of the *tbrA* promoter region (Fig. 7*A*). This construct was then transformed into BMB171, resulting in recombinant BMB-TbrB-GFP expressing a TbrB-GFP fusion protein. As shown in Fig. 7*B*, an obvious green fluorescent signal indicating TbrB-GFP localization appeared specifically at the cell membrane of BMB-TbrB-GFP. In the control, GFP was distributed uniformly inside the cells of BMB-GFP. This result demonstrated that TbrB is a membrane protein of *B. thuringiensis*.

Q-TOF-MS analysis of the intracellular contents of strain BMB2451-Δ*tbrB* revealed the presence of TAA (Fig. 5*C*), indicating active TAA formation despite *tbrB* function *in vivo*. However, TAA presence in the extracellular fraction of BMB2451-Δ*tbrB* was significantly reduced compared with BMB2451, where *tbrB* was functional (Fig. 5*A*). Furthermore, *tbrB* copy number was increased in recombinant BMB2451-*tbrB*, which was constructed based on the BMB2451 strain. This strain showed a substantially higher level of TAA in the culture supernatant than BMB2451 (Fig. 7*C*), in agreement with reports that the introduction of additional transporter genes into metabolite-producing bacteria could significantly promote product yield (49). Together, these results demonstrated a TAA membrane transporter role for the TbrB protein of *B. thuringiensis*.

The Biological Processes of TAA Biosynthesis in B. thuringiensis—TAA biosynthesis through an isomerous pathway in *B. thuringiensis* is proposed in Fig. 8. First, the substrate of aconitate isomerase, CAA, is formed as an intermediate through citric acid dehydration by aconitase (ACO) in the TCA cycle. Instead of being hydrated to isocitric acid by further action of ACO, a portion of CAA is isomerized into TAA by the TbrA protein. Although the isomerization is reversible, TbrA isomerase equilibrium favors TAA. The membrane-anchored TbrB protein transports TAA out of cells, resulting in extracellular accumulation of TAA.

Distribution of TAA Biosynthetic Gene Cluster in the B. cereus Group—To determine whether other *B. cereus* group bacteria have the potential to produce TAA, we investigated the presence of the identified TAA genes in the *B. cereus* group. As shown in Table 3, a 2,097-bp sequence comprising a 1,074-bp *tbrA* ORF sequence, an 111-bp intergenic region, and a 912-bp *tbrB* ORF sequence (Fig. 4*A*) is found in *B. thuringiensis* and *B. cereus* bacteria. All targets are located on plasmids except for strains whose genomes were incomplete. In addition, two transposase genes were found at both ends of the TAA gene cluster (Fig. 4*A*), indicating possible acquisition of the TAA biosynthetic gene cluster by *B. cereus* and *B. thuringiensis* bacteria through horizontal gene transfer.

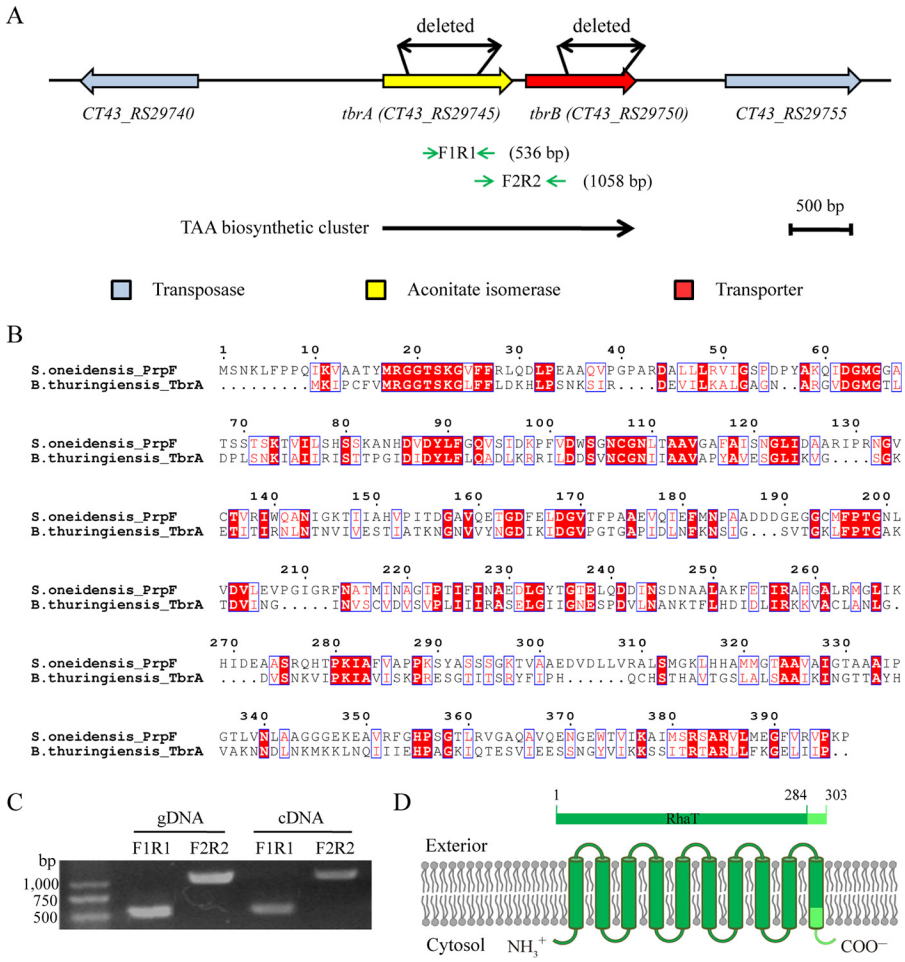

FIGURE 4. **Bioinformatics analysis of putative TAA biosynthesis-related (*tbr*) genes *tbrA* and *tbrB* in *B. thuringiensis* CT-43.** *A*, gene organization of the *tbr* operon region on plasmid pCT281. Two transposase genes are shown in *blue*; putative aconitate isomerase gene *tbrA* and predicted membrane protein gene *tbrB* are shown in *yellow* and *red*, respectively. *Double-headed black arrows* indicate the deleted regions within *tbrA* and *tbrB* ORFs in gene deletion experiments. *Two pairs* of *inverted green arrows* indicate the amplifying regions in the operon analysis experiment of *tbrA* and *tbrB* genes, and the sizes of the amplification products F1R1 and F2R2 are provided. *B*, sequence alignment of TbrA protein of *B. thuringiensis* CT-43 with PrpF protein from *S. oneidensis* MR-1. The alignment was performed using ClustalX and highlighted using ESPript version 3.0. Identical residues are shown in *red*, and residues with similar side chains are *boxed*. *C*, operon analysis of *tbrA* and *tbrB* genes in *B. thuringiensis* CT-43 by reverse transcription PCR. *gDNA*, the genomic DNA of strain CT-43. *D*, schematic of the putative transmembrane protein TbrB. Ten transmembrane helices of TbrB are shown in *green*. The L-rhamnose-H^+ transporter (RhaT) domain that locates at the amino terminus of TbrB protein (aa 1–284) is indicated in *dark green*, and the rest of the carboxyl-terminal sequence (aa 285–303) is shown in *light green*.

Discussion

Despite its relationship to central metabolism, TAA biosynthesis and biofunction have remained unclear since its discovery almost a century ago. In this study, we discovered a novel biological role of TAA (also named CT-A before the structure identification; Fig. 2) as a nematicidal molecule of the *B. thuringiensis* bacterium and revealed how this small metabolite is biosynthesized.

TAA is an unusual cellular metabolite, and thus the fact that *B. thuringiensis* synthesizes and secretes large amounts of TAA suggests a specific purpose (*e.g.* use of TAA as a nematicidal factor). TAA is not necessary for basic biological metabolisms and is known to strongly inhibit the activity of aconitase (25). When intracellular TAA accumulates, the cell must clear it through methylation (50) or transport to avoid inhibition and maintain the normal operation of the TCA cycle. Thus, TAA biosynthesis does not appear to be necessary for central metabolism. With the newly identified nematicidal activity of TAA, we can now reasonably answer why *B. thuringiensis* produces high levels of TAA and reveal it as a novel virulence factor of this nematode pathogen. CAA, which is an essential cellular metabolite, has a pH similar to that of its isomer TAA but displayed a much weaker nematicidal effect (Fig. 3*B*). This further suggests that TAA is a specifically produced molecule whose *trans*-conformation contributes to its nematicidal activity.

We noticed similar effects contributed by the specific *trans*-structure of TAA. For example, *in vitro*, TAA inhibited the growth and transformation of *Leishmania donovani*, the etiological agent of kala-azar, whereas CAA had no effect (51, 52). In barnyard grass, a high endogenous TAA level was revealed to function as an antifeedant of rice brown planthopper, and CAA was determined to be non-functional (33). In addition, TAA has an anti-edematogenic effect (53) that may be due to its unexpected specific inhibitory effect on human phosphodiesterase 7 (PDE7) (54), an inflammatory disease-associated enzyme. Based on these reports, we conclude that TAA is a multifunctional natural product despite its simple molecular structure.

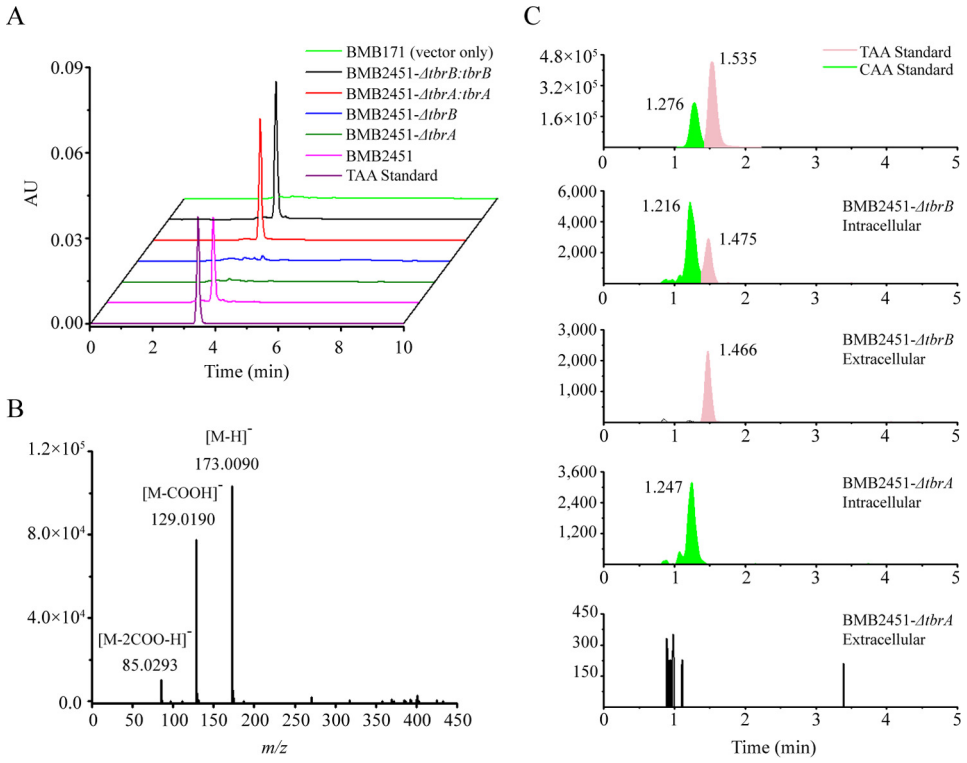

FIGURE 5. **Genetic verification of the TAA biosynthetic gene cluster.** *A*, HPLC analysis of TAA in the culture supernatants of BMB2451 (*pink line*), BMB2451-Δ*tbrA* (*dark green line*), BMB2451-Δ*tbrB* (*blue line*), BMB2451-Δ*tbrA*:*tbrA* (*red line*), and BMB2451-Δ*tbrB*:*tbrB* (*black line*) recombinant strains. TAA standard (*purple line*) and the supernatant extract of BMB171 with empty vector pHT304 (*light green line*) were used as positive and negative controls, respectively. *B*, Q-TOF-MS confirmation of TAA production by heterologous expression of the *tbr* operon in BMB2451. *C*, Q-TOF-MS analysis of TAA presence in intracellular and extracellular fractions of BMB2451-Δ*tbrA* and BMB2451-Δ*tbrB* mutants. The *m*/*z* 173.0090 ion indicating the mass of $[M - H]^-$ patterned aconitic acid was used to extract a TAA signal from the total ion chromatograms (*TIC*). Retention times of extracted CAA (*green peak*) and TAA (*pink peak*) signals are provided. *AU*, absorbance units.

To our knowledge, this is the first report demonstrating the cellular TAA biosynthetic pathway in microorganisms. In 1961, Rao and Altekar (27) proposed the existence of a new enzyme catalyzing the interconversion of aconitates and named it aconitate isomerase. In 1971, Klinman and Rose prepared an aconitate isomerase sample from the total protein of *Pseudomonas putida* cells and determined its kinetic properties (28) and reaction mechanism (55). Since then, *Pseudomonas* has been the only reported TAA-metabolizing bacteria; few studies have focused on identification of relevant DNA determinants or characterization of the TAA biosynthesis pathway. Here, through genetic and biochemical methods, we determined that the hypothetical protein-encoding gene *tbrA* is an aconitate isomerase gene that is responsible for intracellular TAA formation in the *B. thuringiensis* bacterium. For extracellular accumulation, the *tbrB* gene encoding a transporter containing a 10-transmembrane helix is required (Fig. 8). According to Klinman and Rose (28), the molecular mass of the putative aconitate isomerase from *P. putida* was 78 ± 10 kDa, which is significantly larger than the 38.13-kDa mass of TbrA in *B. thuringiensis*. This finding indicates that although they drive the same type of reactions, aconitate isomerases from these two bacteria differ in sequence, suggesting possible species-specific origins. PrpF was proposed to work with an aconitase-like (AcnD) enzyme in the 2-methylcitric acid cycle and to isomerize 2-methyl CAA and 2-methyl TAA (43). Because 2-methyl aconitic acids are not commercially available, the isomerase activity of PrpF protein is unverified. Characterization of the aconitate isomerase function of TbrA, the homologous protein of PrpF, could support the putative 2-methyl aconitate *cis*/*trans*-isomerase role of PrpF protein.

B. thuringiensis and *B. cereus* are *B. cereus* group bacteria that inhabit diverse environments, including soil, freshwater, invertebrates, and insectivorous mammals (56). Compared with *B. subtilis*, a plant-associated bacterium, *B. thuringiensis* and *B. cereus* strains contain more nitrogen metabolism-associated genes than those in carbon metabolism, indicating that their hosts are likely to be animals (57, 58). Nematodes are the most abundant soil metazoans. Most nematodes in soil are bacteria feeders, and generally 90–99% of nematode habitats have high microbial activity (59). Thus, a soil environment represents a suitable place for the interactions of bacteria and nematodes, where diverse virulence factors are produced and operate. The distribution of the TAA biosynthetic gene cluster in *B. thuringiensis* and *B. cereus* (Table 3) suggests the potential to produce high levels of nematicidal TAA in these strains. The transposase genes at both ends of the cluster enable the mobility of the TAA biosynthetic genes. These findings indicate that TAA may contribute to bacteria toxicity, synergistically with other active elements, such as Cry toxins or metalloproteinases, in soil bacteria-nematode interactions. Although the nematicidal mechanism of TAA is unclear, we hypothesized it to be metabolism-associated. TAA inhibition of aconitase would limit isocitric acid production in the TCA cycle (26, 52, 60). The

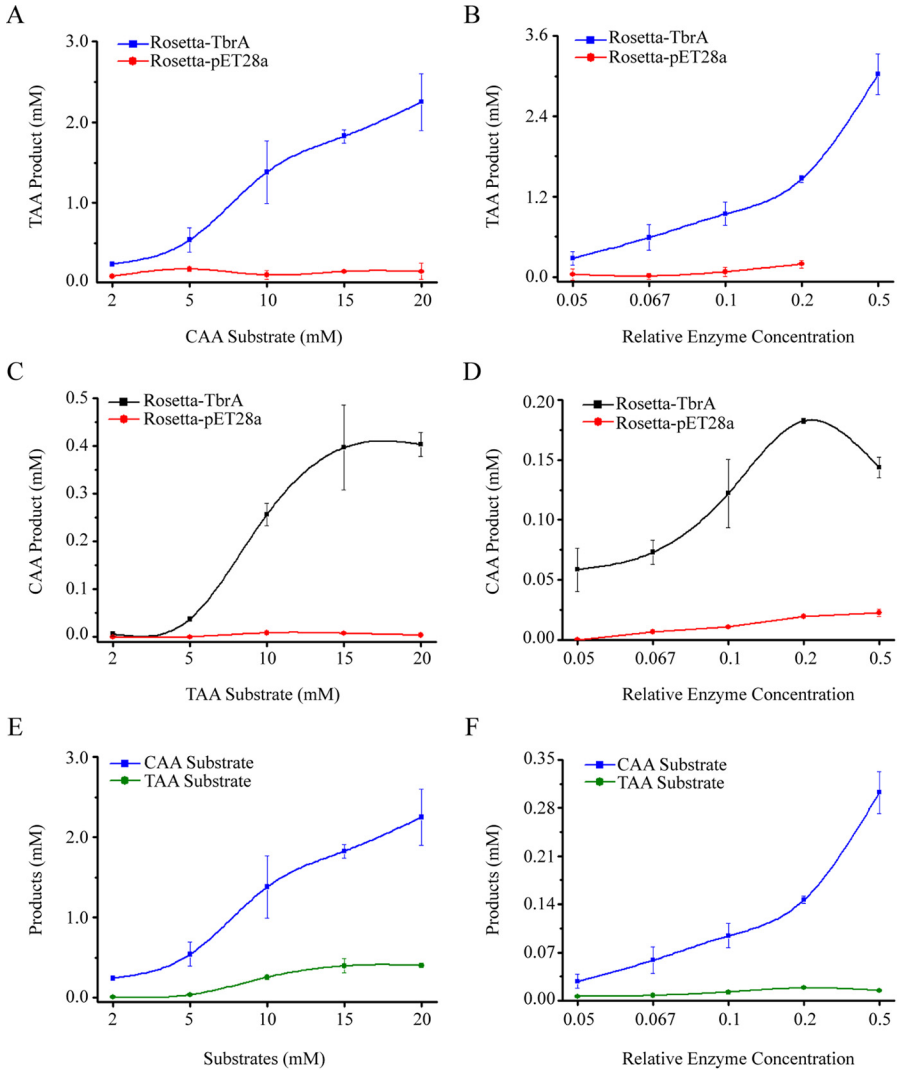

FIGURE 6. **Enzymatic assays of aconitate isomerase activity of TbrA protein.** Cell-free extracts of induced Rosetta-TbrA and Rosetta-pET28a (control) recombinants were used for *in vitro* catalytic reactions. When CAA was used as substrate (*A* and *B*), TAA formation was tested by HPLC with varying CAA substrate concentrations of 2, 5, 10, 15, and 20 mM (*A*) and different relative enzyme concentrations of 0.05, 0.067, 0.1, 0.2, and 0.5 (*B*). Similar assays were performed when TAA was treated as substrate (*C* and *D*). The efficiencies of using CAA and TAA substrates to synthesize TAA and CAA products by TbrA protein were compared with different conditions of substrate (*E*) and enzyme (*F*) concentrations. Data are means ± S.D. (*error bars*).

operation of a glyoxylate shunt, an essential pathway for the survival of parasites during infection (49, 61), may thus be affected in the J2s of *M. incognita*, where the glyoxylate shunt is highly expressed and dependent (62). This is because isocitric acid is a substrate of the first enzyme, isocitrate lyase, in the glyoxylate shunt (49). Combined with the above-mentioned inhibitory effect of TAA on parasite *Leishmania* spp., these facts raise interesting scientific issues, such as whether the glyoxylate shunt can be significantly influenced by TAA or whether TAA has broad activity in glyoxylate shunt-dependent parasites. Although TAA has long been used as an industrial material, these established bioactivities for TAA have potential in promoting its future biological usage in agricultural pest management.

Experimental Procedures

Bacterial Strains, Plasmids, and Culture Conditions—The bacterial strains and plasmids used in the present study are listed in Table 4. All *E. coli* and *B. thuringiensis* strains were cultured in Luria-Bertani (LB) medium at 37 and 28 °C, respectively. When appropriate, antibiotics were added at the following final concentrations: 100 μg/ml ampicillin, 25 μg/ml erythromycin and chloramphenicol, and 50 μg/ml kanamycin.

CT-A (TAA) Extraction, Purification, and Detection—The extraction procedure for crude CT-A (TAA) was identical to that for thuringiensin (21). Samples were stored at 4 °C until use. For CT-A (TAA) purification, sufficient crude sample was first prepared from the CT-43-55 strain over other strains that produce thuringiensin. Purification was carried out using two rounds of preparation with an HPLC system consisting of a Waters 1525 pump, a Waters 2489 UV-visible detector, and a Waters SunFire™ prep C18 OBDTM column (150 × 19 mm, 5 μm; Waters Corp.). In the first round, crude CT-A (TAA) was dissolved in deionized water and carried by a mobile phase containing 10% methanol and 2% acetic acid. The CT-A (TAA) peak was collected and concentrated under reduced pressure using rotary evaporators. Procedures in the second round were

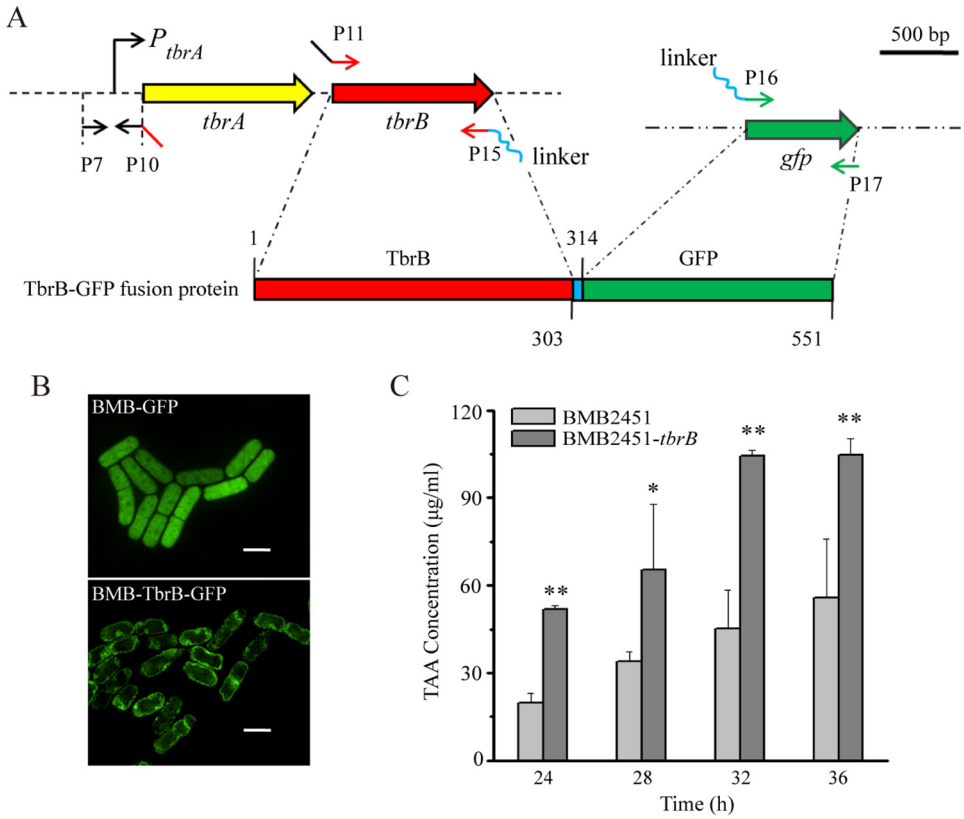

FIGURE 7. **Characterization of TbrB as a TAA transporting membrane protein.** *A*, construction schematic of TbrB-GFP fusion protein. SOE-PCR was performed to connect the promoter region of *tbrA* (P_{tbrA}), the *tbrB* ORF (*red*), a 10-aa peptide linker-encoding sequence (*blue*), and the *gfp* ORF (*green*). Primers are highlighted in *different colors* to indicate individual overlapped regions. *B*, fluorescence image of BMB-TbrB-GFP showed membrane location of TbrB-GFP protein. BMB-GFP cells were used as control. *Scale bar*, 2 μm. *C*, TAA production was substantially promoted in recombinant BMB2451-*tbrB* by introducing additional copies of the *tbrB* gene into BMB2451 (**, $p < 0.01$; *, $p < 0.05$; one-way ANOVA followed by Tukey's honest significant difference test). All data are means ± S.D. (*error bars*).

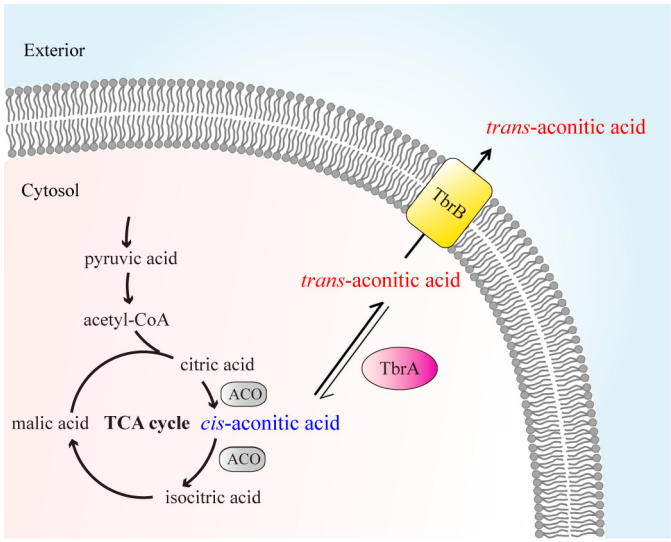

FIGURE 8. **Model of the TAA biosynthetic pathway in *B. thuringiensis*.** The TCA cycle synthesizes CAA through citric acid dehydration by ACO (*gray*). Instead of further hydration to isocitric acid by ACO, a portion of CAA is isomerized into TAA by aconitate isomerase TbrA (*pink*), which catalyzes the reversible reaction from CAA to TAA but favors the equilibrium for TAA, as indicated by the *thicker black arrow*. Intracellular TAA is then transported outside cells by the membrane-anchored TbrB protein (*yellow*), resulting in extracellular accumulation of TAA.

TABLE 3

***B. cereus* group bacteria with TAA biosynthetic gene cluster**

Strain	Location	Identity[a]
		%
B. thuringiensis		
CT-43	pCT281	
YBT-1520	pBMB293	100
HD-1	pBMB299	100
HD-29	pBMB267	100
IS5056	pIS56–285	100
T01-328	—[b]	100
Leapi01	—	100
YC-10	pYC-1	100
Serovar *mexicanensis*	—	100
Serovar *tolworthi*	pKK2	100
B. cereus		
ISP2954	—	100
BMG1.7	—	100
HuB13-1	—	100

[a] Identity between TAA biosynthetic gene cluster of strain CT-43 and predicted genes in other *B. cereus* group bacteria.
[b] —, location undetermined.

similar to the first round, except for the mobile phase (30% acetonitrile and 0.05% formic acid). Finally, the sample was dissolved in deionized water and freeze-dried into powder. The purity of the resulting CT-A (TAA) met the requirements for structure identification, as indicated by a single peak displayed in six HPLC mobile phases (data not shown).

To detect CT-A (TAA) or CAA using HPLC, a similar system was adopted as described above except for the TC-C18 column (250 × 4.6 mm, 5 μm; Agilent). Isocratic elution of a 10-μl sample volume was delivered at a flow rate of 1.0 ml/min and monitored at 260 nm for 10 min. To analyze the sample with LC-MS, a high resolution LC-Q-TOF-MS system was used, which was com-

TABLE 4
Bacterial strains and plasmids used in this study

Strain and plasmid	Description	Source or reference
DH5α	*E. coli* cloning host	Ref. 63
Rosetta-TbrA	*E. coli* Rosetta expressing the TbrA protein	This work
Rosetta-pET28a	*E. coli* Rosetta with empty vector pET28a	This work
CT-43	*B. thuringiensis*, no flagellum; TAA and thuringiensin producer	Refs. 34 and 35
CT-43-55	Strain CT-43 derivative; TAA producer	Ref. 35
CT-43-62	Strain CT-43 derivative; TAA producer	Ref. 35
CT-43-7	Strain CT-43 derivative; thuringiensin producer	Ref. 35
CT-43-1c	Strain CT-43 derivative; thuringiensin producer	Ref. 35
F15	Strain CT-43 derivative; no TAA and thuringiensin production	This work
BMB171	Acrystalliferous mutant of *B. thuringiensis*	Ref. 48
BMB2451	BMB171 with plasmid pBMB2451	This work
BMB2451-Δ*tbrA*	BMB171 with plasmid pBMB2451-Δ*tbrA*	This work
BMB2451-Δ*tbrB*	BMB171 with plasmid pBMB2451-Δ*tbrB*	This work
BMB2451-Δ*tbrA*:*tbrA*	BMB171 with plasmids pBMB2451-Δ*tbrA* and pEMB0603-*tbrA*	This work
BMB2451-Δ*tbrB*:*tbrB*	BMB171 with plasmids pBMB2451-Δ*tbrB* and pEMB0603-*tbrB*	This work
BMB-TbrB-GFP	BMB171 with plasmid pBMB-*tbrB-gfp*	This work
BMB-GFP	BMB171 with plasmid pBMB-*gfp*	This work
BMB2451-*tbrB*	BMB2451 with plasmid pEMB0603-*tbrB*	This work
pHT304	*E. coli–B. thuringiensis* shuttle vector	Ref. 47
pHT304-TS	pHT304 derivative with a temperature-sensitive *Bacillus* replicon	Ref. 21
pMD19-T	*E. coli* cloning vector	Takara
pET28a	*E. coli* expression vector	Takara
pET28a-*tbrA*	TbrA protein expressing plasmid	This work
pEMB0603	*E. coli-B. thuringiensis* shuttle BAC vector	Ref. 39
pEMB0603-*tbrA*	pEMB0603 with intact *tbrA* gene	This work
pEMB0603-*tbrB*	pEMB0603 with *tbrB* ORF fused with *tbrA* gene promoter	This work
pBMB2451	pHT304 carrying *tbrA* and *tbrB* genes	This work
pBMB2451-Δ*tbrA*	*tbrA* gene deleted pBMB2451 derivative	This work
pBMB2451-Δ*tbrB*	*tbrB* gene deleted pBMB2451 derivative	This work
pBMB-*tbrB-gfp*	pHT304 with *tbrB-gfp* fusion gene	This work
pBMB-*gfp*	pHT304 with *gfp* gene	This work

posed of an Agilent 1260 LC device attached to a dual-source electrospray ionization ion source equipped with a G6540A Q-TOF-MS system (Agilent). Samples were analyzed in negative ion mode using diode array detection at 260 nm. Calibration was delivered using standard references with masses of 112.9855 and 1,033.9881 Da. The quadrupole was set to pass ions from m/z 50 to 1,500. Data were analyzed by Agilent MassHunter qualitative analysis software version B.05.00. CAA (Sigma-Aldrich) and TAA (Tokyo Chemical Industry) commercial standards were purchased and used for analysis.

Gene Deletion in B. thuringiensis CT-43—Genes in plasmid pCT281 that were considered CT-A biosynthesis-related are listed in Table 2. Generally, the target fragment harboring candidate genes on pCT281 was first amplified from the CT-43 genome and cloned into the pMD19-T vector (Takara, Dalian, China). By digestion with appropriate restriction enzymes, the central fragment of the inserted DNA was removed and replaced by a digested spectinomycin resistance gene (*spc*^{r}) fragment. The inserted DNA on pMD19-T was cloned into a pHT304-TS vector (21) and electrophoretically introduced to strain CT-43. After culturing at 42 °C, the bacteria were simultaneously incubated on *spc*^{r} and *erm*^{r} solid agar plates to screen for mutants that were resistant to spectinomycin but not erythromycin. Finally, the *in vivo* gene mutation was verified by sequencing.

Identification and Characterization of TAA Biosynthetic Genes—PCR primers used in this study are listed in Table 5. For heterologous expression, a 2,451-bp PCR fragment harboring *tbrA* and *tbrB* genes was cloned into a 6.5-kb *E. coli-B. thuringiensis* shuttle vector pHT304 (47) to yield the pBMB2451 plasmid, which was then transferred into the *B. thuringiensis* host BMB171 (48) to generate the recombinant strain BMB2451. To delete the *tbrA* gene, the inserted 2,451-bp DNA fragment on pBMB2451 was transferred to the 2.7-kb pMD19-T vector at BamHI and SphI sites. Using this recombinant plasmid as template, reverse PCR was performed to generate a DNA product containing an incomplete *tbrA* ORF, the intact *tbrB* ORF, and the vector sequence, which was then digested at the XbaI site introduced by the reverse primers and subjected to self-ligation. The shortened DNA fragment on vector pMD19-T was transferred back to pHT304, resulting in the *tbrA*-deleted plasmid pBMB2451-Δ*tbrA*. Transforming the plasmid pBMB2451-Δ*tbrA* into the BMB171 host generated the mutant BMB2451-Δ*tbrA*. Similar operations were applied to construct the *tbrB*-deleted mutant BMB2451-Δ*tbrB*. For *tbrA* gene complementation, a compatible plasmid (39), recombinant pEMB0603-*tbrA* carrying a 1,868-bp PCR product containing the intact *tbrA* gene, was introduced into BMB2451-Δ*tbrA*, resulting in the complemented strain BMB2451-Δ*tbrA*:*tbrA*. To complement the *tbrB* gene, splicing overlap extension PCR (SOE-PCR) was performed to fuse the promoter region of *tbrA* with *tbrB* ORF, generating a 1,407-bp product that was inserted into pEMB0603. The generated pEMB0603-*tbrB* was introduced into BMB2451-Δ*tbrB*, resulting in the complemented strain BMB2451-Δ*tbrB*:*tbrB*.

In the operon analysis of *tbrA* and *tbrB* genes, the total RNA of strain CT-43 was prepared and reverse-transcribed into cDNA. RT-PCR was carried out with a primer pair designed to span the interval region between the *tbrA* ORF and *tbrB* ORF (Fig. 4*A*). To increase the copy number of the *tbrB* gene based on BMB2451, a recombinant BMB2451-*tbrB* was constructed by introducing the plasmid pEMB0603-*tbrB* into BMB2451. Supernatants of BMB2451 and BMB2451-*tbrB* cultures were sampled at different time points and subjected to TAA extrac-

TABLE 5

Primers used in this study

Restriction sites and a 10-aa peptide linker-encoding sequence in P15 and P16 primers are underlined.

Primer and description	Sequence (5′–3′)
For amplifying *tbr* operon	
P1	TATGGATCCGGATACCAAGTTGTAGGAGGTG
P2	GCCGCATGCGCTAATAGGCTTATTGCTTC
For deleting *tbrA* gene	
P3	TATTCTAGATCCTGGTGTAGTGGAAATTCG
P4	GCCTCTAGAGTCATCCCTAAGATTGCGGT
For deleting *tbrB* gene	
P5	TATTCTAGAAGGGACTAAGAATAGAAAAGG
P6	GCCTCTAGAAGAAGGGCAGCAAGTTCA
For complementing *tbrA* gene	
P7	TATGGATCCCCGTGAAGCGTCTCATCCTAG
P8	GCCAAGCTTCTGCTCTTGTCGCACGTCTCG
For complementing *tbrB* gene	
P9	TATGGATCCCCGTGAAGCGTCTCATCCTAG
P10	GTCGCTTTTTTAAGATTATCCATTTATTAGCATCTCCTTTTTATG
P11	CATAAAAAGGAGATGCTAATAAATGGATAATCTTAAAAAAGCGAC
P12	GCCGCATGCGCTAATAGGCTTATTGCTTC
For analyzing *tbr* operon	
F1	GATTAAAGTCGGGTCAGG
R1	CTGCTGATAATGCGAGCG
F2	TCGCTCGCATTATCAGCAG
R2	TGTCGCACGTCTCGTCTTT
For amplifying *tbrA* ORF	
P13	GGAATTCCATATGATGAAAATACCTTGTTTTGTT
P14	GCCCTCGAGAGGTATTATTAATTCGCCTTT
For constructing *tbrB-gfp* fusion gene (also P7, P10, and P11)	
P15	GCCACCTCCGCCTGAACCGCCTCCACCTGATGAACTTGCTGCCCTTCTTTG
P16	TCAGGTGGAGGCGGTTCAGGCGGAGGTGGCATGAGTAAAGGAGAAG
P17	ACATGCATGCTTATTTGTATAGTTCA
For identifying pCT6880 of strain CT-43	
P6880-1	GCTAACAGCATTAGGTGTGC
P6880-2	GCATATGTGGTGTCGCTTC
For identifying pCT8252 of strain CT-43	
P8252-1	CGATTGAAGAGACGTGTAG
P8252-2	CAGAGGATCTCAATCCTAAG
For identifying pCT8513 of strain CT-43	
P8513-1	CGCAACGATGATGGAAGCA
P8513-2	CATTCTACCTTCAGCATCACC
For identifying pCT9547 of strain CT-43	
P9547-1	GGAATGAGATGGTCGAATC
P9547-2	GCATGTAGAGAACGTACAGC
For identifying pCT14 of strain CT-43	
P14-1	TCGTCAGCATTCATTTGAGC
P14-2	GGGTTATCCGTTATATCCTG
For identifying pCT51 of strain CT-43	
P51-1	CACTGGAATGGTGATGTAGA
P51-2	GTATCAGGCATCTTCTGCAC
For identifying pCT72 of strain CT-43	
P72-1	ATCGGTACAACTGGTTCAGG
P72-2	GATGTTGCGGTATGCTAATC
For identifying pCT83 of strain CT-43	
P83-1	GAAGACGGTAATGGATGAAG
P83-2	GCTGCTATACCAATAGACG
For identifying pCT127 of strain CT-43	
P127-1	CAACGAATGTAGTGAACGG
P127-2	CGTCGCTAGGGTAACTATAG
For identifying pCT281 of strain CT-43	
P281-1	GGAGAGTCTGGATTCGT
P281-2	GCGATGTCACCTATCGTTG

tion as described above. The TAA level was quantified by HPLC and calibrated using the optical density of the cell culture at 600 nm (A_{600}). All of the PCR products amplified in this study were verified by sequencing.

Enzymatic Assay of Aconitate Isomerase Activity of TbrA Protein—The gene *tbrA* was amplified from the genomic DNA of *B. thuringiensis* CT-43 and cloned into NdeI and XhoI sites of the expression vector pET28a to generate a recombinant plasmid pET28a-*tbrA*, which was then transformed into *E. coli* Rosetta to yield a recombinant Rosetta-TbrA for TbrA-inducible expression. The Rosetta-TbrA strain was cultured in 5 ml of LB medium with kanamycin and chloramphenicol at 37 °C for 4 h and transferred into 100 ml of LB medium with an appropriate amount of antibiotics in a ratio of 1:100 and cul-

tured for 3 h, followed by the addition of 0.1 mM isopropyl-β-D-thiogalactoside (final concentration). The TbrA protein was induced at 28 °C for 6 h. Cells were harvested and resuspended in precooled 50 mM Tris-HCl buffer (pH 8.0) with 10% glycerol; the cell-free supernatant of the Rosetta-TbrA strain was collected by centrifugation after high pressure shaking at 4 °C. To test the aconitate isomerase activity of the cell-free extracts of the Rosetta-TbrA strain, CAA and TAA standards (adjusted with 5 M NaOH to pH 7.0) were used as substrates. Two control reactions, one lacking the substrate component and one lacking the cell-free extract component (enzyme), were also performed to calibrate the original presence of TAA and CAA in the cell-free extracts and the non-enzymatic isomerization between the two isomers. The reaction was conducted in a 500-μl test volume at 37 °C for 30 min and terminated by the addition of 20 μl of 6 M HCl. The reaction products were analyzed by HPLC in a mobile phase containing 10% methanol and 0.1% formic acid. The recombinant Rosetta-pET28a harboring the empty vector pET28a was treated with the same induction and culture operations as the negative control strain throughout the enzymatic assays.

Fluorescence Microscopy—SOE-PCR was performed to construct the *tbrB-gfp* fusion gene that comprised the promoter region of *tbrA*, the *tbrB* ORF, a 10-aa peptide linker-encoding sequence, and the *gfp* ORF (Fig. 7*A*). The fusion gene was introduced into host BMB171 by pHT304 vector to generate the recombinant BMB-TbrB-GFP. The bacteria was grown in LB medium at 28 °C for 24 h, and 1 ml of the cell culture was centrifuged, washed with 1× PBS buffer (pH 7.4), and resuspended in 0.5 ml of PBS. The strain BMB171-GFP, which constitutively expresses GFP protein, was used as a control and subjected to the same treatments. Cells were visualized and photographed using a Nikon structured illumination superresolution microscope (N-SIM). Images were processed using NIS-Elements advanced research microscope imaging software.

Nematode Bioassay—The root knot nematodes *M. incognita* were maintained on tomato roots (*Solanum lycopersicum* L., cv. Rutgers). Sixty days after nematode inoculation, egg masses of *M. incognita* were collected and sterilized with sodium hypochlorite and hatched in sterilized deionized water into J2s at 20 °C for 3 days. In the bioassay performed in 96-well plates, each well contained 20–40 J2s in a 100-μl test volume. The nematicidal effects of CT-A (TAA) extracts and CAA and TAA commercial standards were tested. Sterilized deionized water was used as a control. Treatments and bioassays were performed in triplicate. After 72 h, both total and living nematode numbers were recorded.

Bioinformatics Analysis—The antiSMASH database (version 3.0.5) and the batch Conserved Domain Search service (CD-Search) were used to identify secondary metabolite biosynthetic gene clusters and isomerase genes on plasmid pCT281, respectively. The protein sequence alignment of TbrA from *B. thuringiensis* CT-43 and PrpF from *S. oneidensis* MR-1 was performed using ClustalX and highlighted using ESPript version 3.0. The transmembrane helix prediction of the TbrB protein was conducted using the TMHMM Server version 2.0. Protein BLAST and nucleotide BLAST were used to analyze the distribution of the TAA biosynthetic gene cluster among all genome sequences of the *B. cereus* group strains in GenBank™.

Statistical Analysis—One-way ANOVA with Tukey's honest significant difference test was performed to identify statistically significant differences in TAA production by *B. thuringiensis* strains. In nematode bioassays, the LC_{50} values were calculated by probit analysis. IBM SPSS (Statistical Package for the Social Sciences) software version 20.0 was used for these analyses.

Author Contributions—C. D., S. C., and M. S. designed the research. C. D., S. C., X. S., and X. N. performed the experiments and analyzed the data. C. D. wrote the paper. J. Z. and M. S. revised the paper. M. S., D. P., L. R., and Y. D. provided suggestions. All authors reviewed the results and approved the final version of the manuscript.

Acknowledgment—We thank Prof. Q. J. Kang (Shanghai Jiao Tong University) for suggestions on structure identification.

References

1. Peng, D., Lin, J., Huang, Q., Zheng, W., Liu, G., Zheng, J., Zhu, L., and Sun, M. (2016) A novel metalloproteinase virulence factor is involved in *Bacillus thuringiensis* pathogenesis in nematodes and insects. *Environ. Microbiol.* **18,** 846–862
2. Ruan, L., Crickmore, N., Peng, D., and Sun, M. (2015) Are nematodes a missing link in the confounded ecology of the entomopathogen *Bacillus thuringiensis*? *Trends Microbiol.* **23,** 341–346
3. Zheng, J., Peng, D., Chen, L., Liu, H., Chen, F., Xu, M., Ju, S., Ruan, L., and Sun, M. (2016) The *Ditylenchus destructor* genome provides new insights into the evolution of plant parasitic nematodes. *Proc. Biol. Sci.* 10.1098/rspb.2016.0942
4. Luo, X., Chen, L., Huang, Q., Zheng, J., Zhou, W., Peng, D., Ruan, L., and Sun, M. (2013) *Bacillus thuringiensis* metalloproteinase Bmp1 functions as a nematicidal virulence factor. *Appl. Environ. Microbiol.* **79,** 460–468
5. Sanahuja, G., Banakar, R., Twyman, R. M., Capell, T., and Christou, P. (2011) *Bacillus thuringiensis*: a century of research, development and commercial applications. *Plant Biotechnol. J.* **9,** 283–300
6. Bravo, A., Likitvivatanavong, S., Gill, S. S., and Soberón, M. (2011) *Bacillus thuringiensis*: a story of a successful bioinsecticide. *Insect Biochem. Mol. Biol.* **41,** 423–431
7. Zheng, Z., Zheng, J., Zhang, Z., Peng, D., and Sun, M. (2016) Nematicidal spore-forming Bacilli share similar virulence factors and mechanisms. *Sci. Rep.* **6,** 31341
8. Luo, H., Xiong, J., Zhou, Q., Xia, L., and Yu, Z. (2013) The effects of *Bacillus thuringiensis* Cry6A on the survival, growth, reproduction, locomotion, and behavioral response of *Caenorhabditis elegans*. *Appl. Microbiol. Biotechnol.* **97,** 10135–10142
9. Hu, Y., Platzer, E. G., Bellier, A., and Aroian, R. V. (2010) Discovery of a highly synergistic anthelmintic combination that shows mutual hypersusceptibility. *Proc. Natl. Acad. Sci. U.S.A.* **107,** 5955–5960
10. Iatsenko, I., Nikolov, A., and Sommer, R. J. (2014) Identification of distinct *Bacillus thuringiensis* 4A4 nematicidal factors using the model nematodes *Pristionchus pacificus* and *Caenorhabditis elegans*. *Toxins* **6,** 2050–2063
11. Iatsenko, I., Boichenko, I., and Sommer, R. J. (2014) *Bacillus thuringiensis* DB27 produces two novel protoxins, Cry21Fa1 and Cry21Ha1, which act synergistically against nematodes. *Appl. Environ. Microbiol.* **80,** 3266–3275
12. Lenane, I. J., Bagnall, N. H., Josh, P. F., Pearson, R. D., Akhurst, R. J., and Kotze, A. C. (2008) A pair of adjacent genes, *cry5Ad* and *orf2–5Ad*, encode the typical N- and C-terminal regions of a Cry5Aδ-endotoxin as two separate proteins in *Bacillus thuringiensis* strain L366. *FEMS Microbiol. Lett.* **278,** 115–120
13. Liu, Y., Ye, W., Zheng, J., Fang, L., Peng, D., Ruan, L., and Sun, M. (2014) High-quality draft genome sequence of nematocidal *Bacillus thuringiensis* Sbt003. *Stand. Genomic Sci.* **9,** 624–631

14. Salehi Jouzani, G., Seifinejad, A., Saeedizadeh, A., Nazarian, A., Yousefloo, M., Soheilivand, S., Mousivand, M., Jahangiri, R., Yazdani, M., Amiri, R. M., and Akbari, S. (2008) Molecular detection of nematicidal crystalliferous *Bacillus thuringiensis* strains of Iran and evaluation of their toxicity on free-living and plant-parasitic nematodes. *Can. J. Microbiol.* **54,** 812–822
15. Wei, J. Z., Hale, K., Carta, L., Platzer, E., Wong, C., Fang, S. C., and Aroian, R. V. (2003) *Bacillus thuringiensis* crystal proteins that target nematodes. *Proc. Natl. Acad. Sci. U.S.A.* **100,** 2760–2765
16. Li, X. Q., Wei, J. Z., Tan, A., and Aroian, R. V. (2007) Resistance to root-knot nematode in tomato roots expressing a nematicidal *Bacillus thuringiensis* crystal protein. *Plant Biotechnol. J.* **5,** 455–464
17. Li, X. Q., Tan, A., Voegtline, M., Bekele, S., Chen, C. S., and Aroian, R. V. (2008) Expression of Cry5B protein from *Bacillus thuringiensis* in plant roots confers resistance to root-knot nematode. *Biol. Control* **47,** 97–102
18. Zhang, L., Yu, J., Xie, Y., Lin, H., Huang, Z., Xu, L., Gelbic, I., and Guan, X. (2014) Biological activity of *Bacillus thuringiensis* (Bacillales: Bacillaceae) Chitinase against *Caenorhabditis elegans* (Rhabditida: Rhabditidae). *J. Econ. Entomol.* **107,** 551–558
19. Garsin, D. A., Sifri, C. D., Mylonakis, E., Qin, X., Singh, K. V., Murray, B. E., Calderwood, S. B., and Ausubel, F. M. (2001) A simple model host for identifying Gram-positive virulence factors. *Proc. Natl. Acad. Sci. U.S.A.* **98,** 10892–10897
20. Ruan, L., Wang, H., Cai, G., Peng, D., Zhou, H., Zheng, J., Zhu, L., Wang, X., Yu, H., Li, S., Geng, C., and Sun, M. (2015) A two-domain protein triggers heat shock pathway and necrosis pathway both in model plant and nematode. *Environ. Microbiol.* **17,** 4547–4565
21. Liu, X. Y., Ruan, L. F., Hu, Z. F., Peng, D. H., Cao, S. Y., Yu, Z. N., Liu, Y., Zheng, J. S., and Sun, M. (2010) Genome-wide screening reveals the genetic determinants of an antibiotic insecticide in *Bacillus thuringiensis*. *J. Biol. Chem.* **285,** 39191–39200
22. Noel, G. R. (1990) Evaluation of thuringiensin for control of *Heterodera glycines* on soybean. *J. Nematol.* **22,** 763–766
23. Liu, X., Ruan, L., Peng, D., Li, L., Sun, M., and Yu, Z. (2014) Thuringiensin: a thermostable secondary metabolite from *Bacillus thuringiensis* with insecticidal activity against a wide range of insects. *Toxins* **6,** 2229–2238
24. Altekar, W. W., and Rao, M. R. (1963) Microbiological dissimilation of tricarballylate and *trans*-aconitate. *J. Bacteriol.* **85,** 604–613
25. Saffran, M., and Prado, J. L. (1949) Inhibition of aconitase by *trans*-aconitate. *J. Biol. Chem.* **180,** 1301–1309
26. Sugimoto, T., Kato, T., and Park, E. Y. (2014) Functional analysis of *cis*-aconitate decarboxylase and *trans*-aconitate metabolism in riboflavin-producing filamentous *Ashbya gossypii*. *J. Biosci. Bioeng.* **117,** 563–568
27. Rao, M. R., and Altekar, W. W. (1961) Aconitate isomerase. *Biochem. Biophys. Res. Commun.* **4,** 101–105
28. Klinman, J. P., and Rose, I. A. (1971) Purification and kinetic properties of aconitate isomerase from *Pseudomonas putida*. *Biochemistry* **10,** 2253–2259
29. Thompson, J. F., Schaefer, S. C., and Madison, J. T. (1990) Determination of aconitate isomerase in plants. *Anal. Biochem.* **184,** 39–47
30. Thompson, J. F., Schaefer, S. C., and Madison, J. T. (1997) Role of aconitate isomerase in *trans*-aconitate accumulation in plants. *J. Agric. Food Chem.* **45,** 3684–3688
31. Brauer, D., and Teel, M. R. (1981) Metabolism of *trans*-aconitic acid in maize: I. purification of two molecular forms of citrate dehydrase. *Plant Physiol.* **68,** 1406–1408
32. Miller, R. E., and Cantor, S. M. (1951) Aconitic acid, a by-product in the manufacture of sugar. *Adv. Carbohydr. Chem.* **6,** 231–249
33. Kim, M., Koh, H. S., Obata, T., Fukami, H., and Ishii, S. (1976) Isolation and identification of *trans*-aconitate as the antifeedant in barnyard grass against the brown planthopper *Nilaparvata Lugens* (Stål) (Homoptera: Delphacidae). *Appl. Ent. Zool.* **11,** 53–57
34. He, J., Wang, J., Yin, W., Shao, X., Zheng, H., Li, M., Zhao, Y., Sun, M., Wang, S., and Yu, Z. (2011) Complete genome sequence of *Bacillus thuringiensis* subsp. *chinensis* strain CT-43. *J. Bacteriol.* **193,** 3407–3408
35. Sun, M., and Yu, Z. (1996) Characterization of insecticidal crystal proteins of *Bacillus thuringiensis* subsp. *chinensis* CT-43. *Acta Microbiologica Sinica* **36,** 303–306
36. Abad, P., Gouzy, J., Aury, J. M., Castagnone-Sereno, P., Danchin, E. G., Deleury, E., Perfus-Barbeoch, L., Anthouard, V., Artiguenave, F., Blok, V. C., Caillaud, M. C., Coutinho, P. M., Dasilva, C., De Luca, F., Deau, F., *et al.* (2008) Genome sequence of the metazoan plant-parasitic nematode *Meloidogyne incognita*. *Nat. Biotechnol.* **26,** 909–915
37. Jones, J. T., Haegeman, A., Danchin, E. G., Gaur, H. S., Helder, J., Jones, M. G., Kikuchi, T., Manzanilla-López, R., Palomares-Rius, J. E., Wesemael, W. M., and Perry, R. N. (2013) Top 10 plant-parasitic nematodes in molecular plant pathology. *Mol. Plant Pathol.* **14,** 946–961
38. Smith, C. A., O'Maille, G., Want, E. J., Qin, C., Trauger, S. A., Brandon, T. R., Custodio, D. E., Abagyan, R., and Siuzdak, G. (2005) METLIN, a metabolite mass spectral database. *Ther. Drug Monit.* **27,** 747–751
39. Luo, Y., Ruan, L. F., Zhao, C. M., Wang, C. X., Peng, D. H., and Sun, M. (2011) Validation of the intact zwittermicin A biosynthetic gene cluster and discovery of a complementary resistance mechanism in *Bacillus thuringiensis*. *Antimicrob. Agents Chemother.* **55,** 4161–4169
40. Blin, K., Medema, M. H., Kottmann, R., Lee, S. Y., and Weber, T. (2017) The antiSMASH database, a comprehensive database of microbial secondary metabolite biosynthetic gene clusters. *Nucleic Acids Res.* **45,** D555–D559
41. Bernheim, F. (1928) The specificity of the dehydrases. *Biochem. J.* **22,** 1178–1192
42. Marchler-Bauer, A., and Bryant, S. H. (2004) CD-Search: protein domain annotations on the fly. *Nucleic Acids Res.* **32,** W327–W331
43. Grimek, T. L., and Escalante-Semerena, J. C. (2004) The *acnD* Genes of *Shewenella oneidensis* and *Vibrio cholerae* encode a new Fe/S-dependent 2-methylcitrate dehydratase enzyme that requires *prpF* Function *in vivo*. *J. Bacteriol.* **186,** 454–462
44. Garvey, G. S., Rocco, C. J., Escalante-Semerena, J. C., and Rayment, I. (2007) The three-dimensional crystal structure of the PrpF protein of *Shewanella oneidensis* complexed with *trans*-aconitate: insights into its biological function. *Protein Sci.* **16,** 1274–1284
45. Tate, C. G., Muiry, J. A., and Henderson, P. J. (1992) Mapping, cloning, expression, and sequencing of the *rhaT* gene, which encodes a novel L-rhamnose-H^+ transport protein in *Salmonella typhimurium* and *Escherichia coli*. *J. Biol. Chem.* **267,** 6923–6932
46. Tate, C. G., and Henderson, P. J. (1993) Membrane topology of the L-rhamnose-H^+ transport protein (RhaT) from Enterobacteria. *J. Biol. Chem.* **268,** 26850–26857
47. Arantes, O., and Lereclus, D. (1991) Construction of cloning vectors for *Bacillus thuringiensis*. *Gene* **108,** 115–119
48. He, J., Shao, X., Zheng, H., Li, M., Wang, J., Zhang, Q., Li, L., Liu, Z., Sun, M., Wang, S., and Yu, Z. (2010) Complete genome sequence of *Bacillus thuringiensis* mutant strain BMB171. *J. Bacteriol.* **192,** 4074–4075
49. Cordes, T., Michelucci, A., and Hiller, K. (2015) Itaconic acid: the surprising role of an industrial compound as a mammalian antimicrobial metabolite. *Annu. Rev. Nutr.* **35,** 451–473
50. Cai, H., and Clarke, S. (1999) A novel methyltransferase catalyzes the methyl esterification of *trans*-aconitate in *Escherichia coli*. *J. Biol. Chem.* **274,** 13470–13479
51. Misra, S., Sanyal, T., Sarkar, D., Bhattacharya, P. K., and Ghosh, D. K. (1989) Evaluation of antileishmanial activity of *trans*-aconitic acid. *Biochem. Med. Metab. Biol.* **42,** 171–178
52. Kar, S., Kar, K., Bhattacharya, P. K., and Ghosh, D. K. (1993) Experimental visceral leishmaniasis: role of *trans*-aconitic acid in combined chemotherapy. *Antimicrob. Agents Chemother.* **37,** 2459–2465
53. Garcia Ede, F., de Oliveira, M. A., Godin, A. M., Ferreira, W. C., Bastos, L. F., Coelho Mde, M., and Braga, F. C. (2010) Antiedematogenic activity and phytochemical composition of preparations from *Echinodorus grandiflorus* leaves. *Phytomedicine* **18,** 80–86
54. Chen, S. T., Lee, I. S., and Chen, Y. C. (April 6, 2015) *Trans*-aconitic acid compounds and uses thereof for inhibiting phosphodiesterase 7. U. S. Patent 20150104531
55. Klinman, J. P., and Rose, I. A. (1971) Mechanism of the aconitate isomerase reaction. *Biochemistry* **10,** 2259–2266

56. Raymond, B., Johnston, P. R., Nielsen-LeRoux, C., Lereclus, D., and Crickmore, N. (2010) *Bacillus thuringiensis*: an impotent pathogen? *Trends Microbiol.* **18,** 189–194
57. Zhu, L., Peng, D., Wang, Y., Ye, W., Zheng, J., Zhao, C., Han, D., Geng, C., Ruan, L., He, J., Yu, Z., and Sun, M. (2015) Genomic and transcriptomic insights into the efficient entomopathogenicity of *Bacillus thuringiensis*. *Sci. Rep.* **5,** 14129
58. Ivanova, N., Sorokin, A., Anderson, I., Galleron, N., Candelon, B., Kapatral, V., Bhattacharyya, A., Reznik, G., Mikhailova, N., Lapidus, A., Chu, L., Mazur, M., Goltsman, E., Larsen, N., D'Souza, M., *et al.* (2003) Genome sequence of *Bacillus cereus* and comparative analysis with *Bacillus anthracis*. *Nature* **423,** 87–91
59. Zhou, J., Li, X., Jiang, Y., Wu, Y., Chen, J., Hu, F., and Li, H. (2011) Combined effects of bacterial-feeding nematodes and prometryne on the soil microbial activity. *J. Hazard. Mater.* **192,** 1243–1249
60. Middendorf, P. J., and Dusenbery, D. B. (1993) Fluoroacetic acid is a potent and specific inhibitor of reproduction in the nematode *Caenorhabditis elegans*. *J. Nematol.* **25,** 573–577
61. McKinney, J. D., Höner zu Bentrup, K., Muñoz-Elías, E. J., Miczak, A., Chen, B., Chan, W. T., Swenson, D., Sacchettini, J. C., Jacobs, W. R., Jr., and Russell, D. G. (2000) Persistence of *Mycobacterium tuberculosis* in macrophages and mice requires the glyoxylate shunt enzyme isocitrate lyase. *Nature* **406,** 735–738
62. Lourenço-Tessutti, I. T., Souza Junior, J. D., Martins-de-Sa, D., Viana, A. A., Carneiro, R. M., Togawa, R. C., de Almeida-Engler, J., Batista, J. A., Silva, M. C., Fragoso, R. R., and Grossi-de-Sa, M. F. (2015) Knock-down of heat-shock protein 90 and isocitrate lyase gene expression reduced root-knot nematode reproduction. *Phytopathology* **105,** 628–637
63. Hanahan, D. (1983) Studies on transformation of *Escherichia coli* with plasmids. *J. Mol. Biol.* **166,** 557–580